

MASS TRANSFER IN CLOSE, RAPIDLY ACCRETING PROTOBINARIES: AN ORIGIN FOR MASSIVE TWINS?

MARK R. KRUMHOLZ¹ AND TODD A. THOMPSON²

Department of Astrophysical Sciences, Princeton University, Princeton, NJ 08544; krumholz@astro.princeton.edu, thomp@astro.princeton.edu

Received 2006 November 22; accepted 2007 February 19

ABSTRACT

Rapidly accreting massive protostars undergo a phase of deuterium shell burning during pre-main-sequence evolution that causes them to swell to tenths of an AU in radius. During this phase, those with close binary companions will overflow their Roche lobes and begin transferring mass. Since massive stars frequently have companions at distances well under 1 AU, this process may affect the early evolution of a substantial fraction of massive stars. We use a simple protostellar evolution model to determine the range in accretion rates, mass ratios, and orbital separations for which mass transfer will occur, and we compute approximately the stability and final outcome of the transfer process. We discuss how mass transfer affects the demographics of massive binaries and show that it provides a natural explanation for the heretofore unexplained population of massive “twins,” high-mass binaries with mass ratios very close to unity.

Subject headings: accretion, accretion disks — binaries: close — binaries: spectroscopic — stars: evolution — stars: formation — stars: pre-main-sequence

1. INTRODUCTION

Massive stars form in regions of high pressure and density that produce high accretion rates. Simple order-of-magnitude estimates for the properties of observed massive protostellar cores suggest that accretion rates of $\sim 10^{-4}$ – $10^{-2} M_{\odot} \text{ yr}^{-1}$ are typical (Krumholz 2006), and both detailed analytic models (McKee & Tan 2003) and numerical simulations (Banerjee & Pudritz 2007; Krumholz et al. 2007) produce accretion rates in this range. Observations of protostellar outflows with mass fluxes up to $\sim 10^{-2} M_{\odot} \text{ yr}^{-1}$ from luminous embedded protostars (Henning et al. 2000) also suggest high accretion rates.

The combination of rapid accretion and high mass produces protostars with very large radii, for two reasons. First, Stahler (1988) shows that prior to the onset of deuterium burning, the radius of an accreting protostar is determined primarily by the specific entropy of the gas after it passes through the accretion shock, radiates and settles onto the surface, and is eventually buried in enough optical depth to prevent it from radiating further. A high accretion rate reduces the amount of time an accreted gas element has to radiate before it is buried and thus produces higher specific entropy and larger radius. Second, Palla & Stahler (1991, 1992) show that after deuterium burning begins, massive protostars pass through a period of shell burning. This occurs because as contraction raises the core temperature the opacity decreases to the point where the core becomes convectively stable. Accreting deuterium cannot penetrate the radiative core and, as a result, deuterium burning occurs in a shell around it. In a process analogous to that in a red giant, this produces rapid expansion of the envelope above the burning layer. Together, these two effects can produce radii of several tenths of an AU during the pre-main-sequence evolution of rapidly accreting stars.

Large radii create the possibility of mass transfer in close binaries. Most massive stars appear to be in multiple systems (e.g., Preibisch et al. 2001; Shatsky & Tokovinin 2002; Lada 2006). While the semimajor axis distribution of massive stars is

not well determined, due to low statistics and complex selection biases, there appears to be a significant population of very close binaries. The WR 20a system, the most massive binary known, has a separation of only 0.25 AU (Bonanos et al. 2004; Rauw et al. 2005). The semimajor axis of the massive detached eclipsing binary D33 J013346.2+304439.9 in M33 is 0.22 AU (Bonanos et al. 2006). Harries et al. (2003) and Hilditch et al. (2005) report a sample of 50 OB star eclipsing binaries with periods of 5 days or less taken from the Optical Gravitational Lens Experiment survey (OGLE; Udalski et al. 1998) of the SMC. This period limit corresponds to a semimajor axis of $0.26 M_{100}^{1/3}$ AU, where M_{100} is the total mass in units of $100 M_{\odot}$. Roughly half the systems are detached binaries, indicating that they have not yet undergone any post-main-sequence mass transfer. It is therefore likely that these systems formed at close to their current separations, or possibly even closer, since conservation of energy dictates that mass loss from winds during main-sequence evolution widens the orbits of massive binaries. This means that systems such as WR 20a, D33 J013346.2+304439.9, and the SMC binaries almost certainly experienced a phase of mass transfer during their pre-main-sequence evolution.

To study how this process will affect massive binaries, we proceed as follows. We assume that a “seed” close protobinary system forms while the system is still embedded and accreting. Such a binary may form via one of two possible mechanisms that have been proposed: direct fragmentation of a massive molecular cloud core and subsequent capture of two protostars into a tight binary (e.g., Bonnell & Bate 2005) or fragmentation of a disk around a massive protostar and subsequent migration of a stellar-mass fragment inward (e.g., Kratter & Matzner 2006; Krumholz et al. 2007). Although these two mechanisms arise in the context of specific star formation models, we emphasize that seed binaries of this sort are expected to form early in massive protostars’ lives, in the context of any model where massive protostars form by accretion (e.g., McKee & Tan 2003; Keto & Wood 2006; Krumholz et al. 2007). Moreover, recent observations by Apai et al. (2007) show that massive stars have a high intrinsic binary fraction even while they are still embedded, providing observational support for this hypothesis. It is worth noting, however, that stable binaries

¹ Hubble Fellow.

² Lyman Spitzer Jr. Fellow.

may not form until much later in massive protostellar evolution if massive stars form by collisions (e.g., Bonnell et al. 1998), since binary orbits will suffer continual disruption as long as close encounters leading to mergers are occurring. If massive stars form primarily by collisions and not by accretion, the calculations we present in this paper will not apply.

Given a seed binary, in this paper we calculate how pre-main-sequence stellar evolution and mass transfer will modify its properties. In § 2, we determine the range of parameters for which mass transfer can occur, and in § 3 we discuss the outcome of mass transfer when it does occur. We discuss the implications of this process for the massive binary population, and related points, in § 4, and we summarize our conclusions in § 5.

2. THE PROPERTIES OF MASS TRANSFER BINARIES

The problem of prestellar binary evolution depends on both the accretion histories of the stars and on the properties of their orbit. Even if we limit ourselves to protostars accreting at constant rates and moving in circular orbits of constant size, there are four parameters: the accretion rates onto each of the two stars, the offset in time between formation of the two stars, and the semimajor axis of the orbit. Since fully exploring this parameter space would be time consuming and not particularly informative, we further simplify it by assuming that the two binary components form coevally or nearly so, reducing the space to three dimensions. Our goal is simply to map out for what ranges of accretion rate and orbital separation mass transfer is a possibility. Our assumption that the two components of the binary are roughly coeval and that the larger component has a higher time-averaged accretion rate (necessarily the case for coeval, constant accretion rate systems) is supported by recent simulations of massive star formation (Krumholz et al. 2007).

The first step in exploring this parameter space is to determine the protostellar mass-radius relation as a function of accretion rate, which we do in § 2.1. Using these tracks, in § 2.2 we determine the minimum semimajor axis required for Roche lobe overflow (RLOF) to occur in a binary system consisting of two stars of mass M_1 and M_2 , $M_1 > M_2$, with secondary-to-primary mass ratio $q = M_2/M_1 \leq 1$, orbiting with semimajor axis a . The total system mass is M , and the binary accretes at a rate \dot{M}_{acc} . Under our assumption of coeval formation, the ratio of accretion rates onto the two components is $\dot{M}_{2,\text{acc}}/\dot{M}_{1,\text{acc}} = M_2/M_1 = q$, where the subscript “acc” indicates the change in mass due to accretion into the system, rather than transfer between the two stars.

2.1. The Protostellar Mass-Radius Relation

For a given accretion rate onto a star, we construct a track of radius versus mass using a simple protostellar model. To allow quick exploration of a large range of parameters, we use the one-zone model of McKee & Tan (2003) to generate our tracks. This model has been calibrated against the detailed numerical calculations of Palla & Stahler (1992) and agrees to within $\sim 10\%$. We refer readers to McKee & Tan for a detailed description of the model, but here we summarize its most important features. In this model, a protostar is assumed to be a polytropic sphere with a specified accretion rate as a function of time. At every time step of model evolution, one uses conservation of energy to determine the new radius, including the effects of energy lost in dissociating and ionizing incoming gas, energy radiated away, and energy gained by Kelvin-Helmholtz contraction, deuterium burning, and the gravitational potential energy of accreting gas.

An accreting massive protostar passes through four distinct phases of evolution before reaching the zero-age main sequence (ZAMS). When the star first forms, it evolves passively without

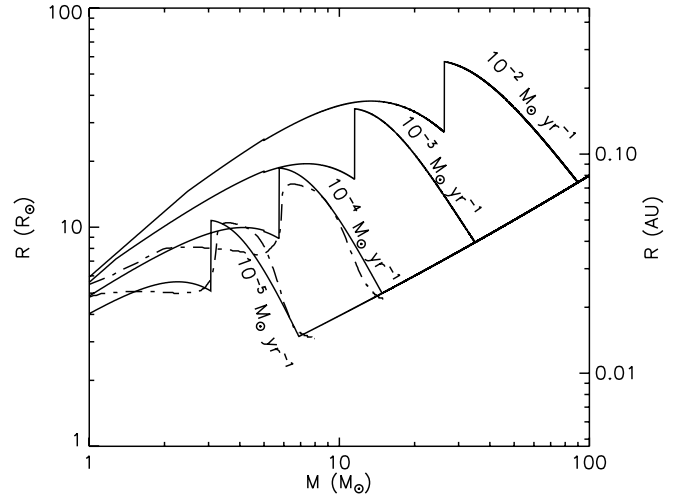


FIG. 1.—Radius vs. mass for constant accretion rates of 10^{-5} – $10^{-2} M_{\odot} \text{ yr}^{-1}$ (solid lines), computed using the simple one-zone McKee & Tan (2003) model. For comparison, we also show the results of the detailed numerical calculation of Palla & Stahler (1991, 1992) for accretion rates of 10^{-5} and $10^{-4} M_{\odot} \text{ yr}^{-1}$ (dot-dashed lines). The sharp rise in R that all models show results from the start of shell deuterium burning.

any nuclear burning. When its core becomes hot enough ($\sim 10^6$ K), the second phase begins: deuterium ignites, the star becomes fully convective and begins burning its accumulated deuterium reserve, and contraction of the core temporarily halts. Once the star exhausts its deuterium reserve, it enters a third phase in which it continues burning deuterium at the rate it is brought in by new accretion. In this phase, the core resumes quasi-static contraction. As the core temperature continues to rise, its opacity drops, and eventually a layer forms that is stable against convection, initiating the fourth phase. Newly accreted deuterium cannot pass through the radiative layer to reach the core, and without an influx of new deuterium, the core rapidly exhausts its supply and becomes convectively stable as well. Deuterium begins burning in a shell above the radiative zone, driving a rapid expansion of the star. As the core continues contracting, the radiative zone increases in size and the star resumes contraction. Eventually the core becomes hot enough to ignite hydrogen, and at that point the star joins the ZAMS.

Figure 1 shows some sample tracks of radius versus mass computed using this model. The sharp increase in radius that each model shows is the result of the start of deuterium shell burning. As the plots show, for the high accretion rates expected in massive star-forming regions, the radius can reach several tenths of an AU. We compute protostellar models for 600 values of \dot{M}_{acc} , uniformly spaced in logarithm in the range 10^{-5} – $10^{-2} M_{\odot} \text{ yr}^{-1}$, accreting up to a maximum mass of $100 M_{\odot}$. By this mass, stars have joined the ZAMS regardless of their accretion rate.

2.2. Roche Lobe Overflow

Having determined the protostellar mass-radius relation, we can now determine for what semimajor axes a a binary of mass ratio q (secondary-to-primary) will experience RLOF. The radius of the Roche lobe around star 1 is (Eggleton 1983)

$$R_{r,1} \approx a \frac{0.49}{0.6 + q^{2/3} \log(1 + q^{-1/3})}; \quad (1)$$

the Roche lobe radius around star 2 is given by an analogous expression with q replaced by q^{-1} . For a given value of q and

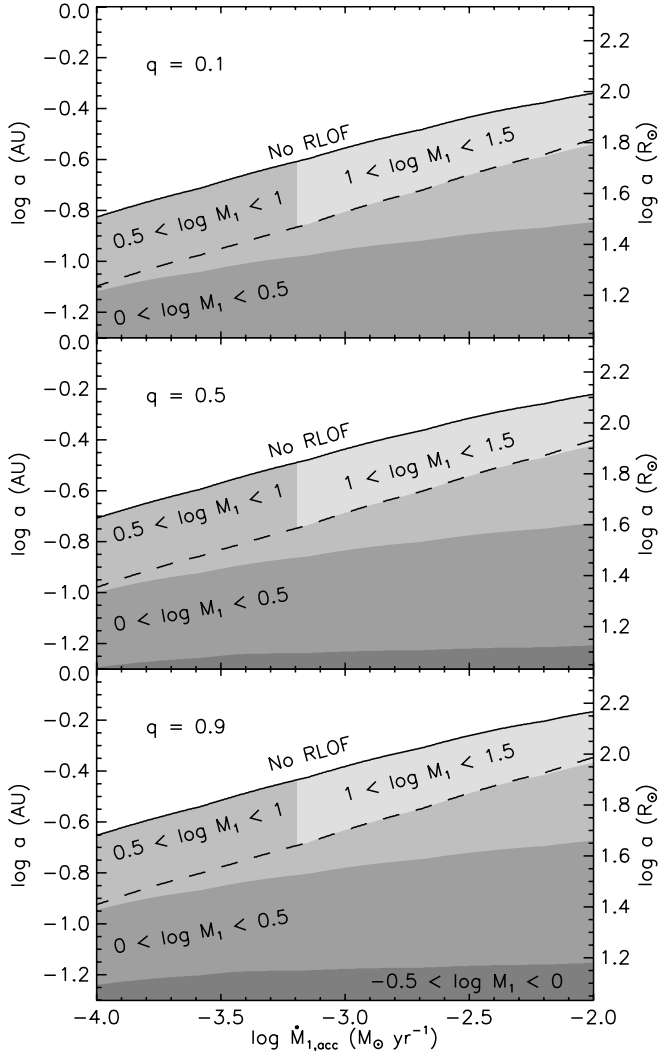


FIG. 2.—Minimum a for RLOF (solid line) as a function of accretion rate onto the more massive star, $\dot{M}_{1,\text{acc}}$. The value of q is indicated in each panel. Below the RLOF line, in the region of parameter space where overflow occurs, we show the mass M_1 (in solar units) of the donor star at overflow (shaded regions). Binaries with a below the dashed line experience overflow before the primary starts deuterium shell burning, while those with larger values of a experience overflow after the onset of shell burning.

$\dot{M}_{1,\text{acc}}$, the accretion rate onto the more massive star, it is straightforward to use the mass-radius tracks to compute whether RLOF ever occurs for a given value of a , and if so, to determine the mass and state of each star when it does.

Figure 2 summarizes the results for three different values of q . We find that in rapidly accreting systems, RLOF will occur when the primary star is $M_1 \gtrsim 10 M_\odot$ and the semimajor axis a is a few tenths of an AU or less; a rough analytic estimate for the critical value of a below which RLOF occurs is

$$a_{\text{crit}} \approx 0.2 \dot{M}_{-4}^{1/4} (1+q)^{1/3} \text{ AU}, \quad (2)$$

where $\dot{M}_{-4} = \dot{M}_{1,\text{acc}}/10^{-4} M_\odot \text{ yr}^{-1}$. Thus, in the context of the model proposed here, observed systems, such as WR 20a, D33 J013346.2+304439.9, and the eclipsing binaries in the SMC, with masses $>20 M_\odot$ and separations $\lesssim 0.25$ AU are well within the expected overflow range for reasonable accretion rates and initial mass ratios. We further find that it is always the more

massive star that overflows its Roche lobe, rather than the less massive one. This is because despite the larger Roche radius around the more massive star, its higher accretion rate leads this star to have a larger radius before the onset of shell burning and to start deuterium shell burning sooner. Finally, note that much of the parameter space allowed for transfer—the region between the dashed and solid lines in Figure 2—is due to the shell-burning phase, which roughly doubles the radius of the star and therefore doubles the minimum value of a for which transfer can occur.

If we were to relax our assumption that the stars are coeval, our conclusion would be strengthened, because simulations indicate that in massive binary systems, the more massive companion generally forms earlier (Krumholz et al. 2007). Since the mass at which deuterium shell burning starts increases with accretion rate (see Fig. 1), and the protostellar radius at any time increases with both mass and accretion rate, this general result should be robust.

3. THE OUTCOME OF ROCHE LOBE OVERFLOW

3.1. Timescales

Before we attempt to calculate the outcome of RLOF, it is helpful to review some relevant timescales for the problem. The shortest is the orbital period, $P = 3.7 a_{0.1}^{3/2} M_{10}^{-1/2}$ days, where $a_{0.1}$ is the semimajor axis in units of 0.1 AU and M_{10} is the total system mass in units of $10 M_\odot$. This is the timescale on which mass lost from the primary star will reach the vicinity of the secondary; actual accretion may take longer if the gas has to be processed through a disk. Next is the dynamical, sound-crossing time of the donor star. The sound speed varies greatly from the stellar core to the surface, so to be conservative and obtain the longest possible timescale, we evaluate this using the surface sound speed, which gives $\tau_{\text{dyn}} = R_{*1}/c_{s,\text{surf}} \sim 31 R_{50} T_4^{-1/2}$ days, where R_{50} is the stellar radius in units of $50 R_\odot$ and T_4 is the stellar surface temperature in units of 10^4 K. The timescale τ_{dyn} describes the time required for the star to adjust mechanically as it loses mass. Finally, there is the Kelvin-Helmholtz time of the donor star, $\tau_{\text{KH}} \sim GM_1^2/(R_{*1}L_1) \sim 6200 M_{10}^2 R_{50}^{-1} L_4^{-1}$ yr, where L_4 is the star's luminosity in units of $10^4 L_\odot$. This describes the time required for the star to adjust thermally to mass loss.

The most important point to take from this calculation is that τ_{KH} is by far the largest timescale in the problem, so that stars will be unable to adjust their thermal (as opposed to mechanical) structure to mass transfer that occurs on orbital or dynamical timescales. Thus, we may approximate stars as behaving adiabatically during mass transfer. A corollary of this is that as gas in the donor star expands adiabatically in response to mass loss, deuterium burning will slow dramatically, since the burning rate is extremely temperature sensitive. Thus, once the star overflows its Roche lobe, its envelope will not have its specific entropy altered by further nuclear burning on a dynamical timescale.

3.2. Stability of Mass Transfer

We first address the question of whether the RLOF leads to stable or unstable mass transfer. Transfer is stable if adiabatic mass loss shrinks the star at a rate faster than the Roche lobe around it shrinks, and is unstable otherwise. If the transfer is unstable, the donor star can change its mass by order unity on a timescale τ_{dyn} , and transfer will stop only when a new mechanical equilibrium is established.

To check stability, we must evaluate how mass transfer changes both the Roche radius and the stellar radius. The former is easy to compute. If no mass is lost from the system, then conservation

of angular momentum demands that the radius of the system shrink at a rate

$$\frac{\dot{a}}{a} = -2 \frac{\dot{M}_1}{M_1} \left(1 - \frac{1}{q_0}\right), \quad (3)$$

where q_0 is the secondary-to-primary mass ratio at the time when mass transfer begins, and \dot{M}_1 is the rate of change of the primary's mass due to mass transfer (as opposed to accretion onto the system). Since $\dot{M}_1 < 0$ and $q_0 < 1$, this means that $\dot{a} < 0$; the semimajor axis of the orbit shrinks in response to mass transfer. From equation (1), the Roche radius around the primary star varies approximately as

$$\frac{\dot{R}_{r1}}{R_{r1}} \approx \frac{\dot{M}_1}{M_1} (1 - q_0) \times \left[\frac{2}{q_0} + \frac{2 \log(1 + q_0^{-1/3}) - (1 + q_0^{1/3})^{-1}}{1.8q_0^{1/3} + 3q_0 \log(1 + q_0^{-1/3})} \right]. \quad (4)$$

The expression in square brackets is always positive for $q_0 < 1$, so the Roche radius around the donor star shrinks as well.

For the range of parameter space we explore, a star undergoing RLOF does so before reaching the ZAMS, and at a mass below $30 M_\odot$. Thus, the star is gas pressure-dominated, at least in its outer layers. If RLOF occurs before the onset of deuterium shell burning, the star is convective throughout and thus is well described as an isentropic $n = 3/2$ polytrope. Since a star with this structure expands in response to mass loss at constant entropy (see below), we learn immediately that RLOF will be unstable in this case, because the star expands as the Roche radius contracts. Thus, systems whose parameters fall below the dashed lines in Figure 2 are always unstable.

If RLOF occurs after deuterium shell burning starts, the star consists of a lower specific entropy inner radiative zone and a significantly larger, high specific entropy envelope. Shell burning eventually raises the temperature in the envelope to the point where it becomes radiative as well (Palla & Stahler 1991), but at the onset of shell burning it is still convective. RLOF occurs at the start of shell burning, since this is the point of maximum radius, so the envelope will also be an isentropic $n = 3/2$ polytrope, with a different specific entropy than the interior radiative zone.

Following the analysis of Paczyński & Sienkiewicz (1972) for a red giant, we can approximate this configuration in terms of a ‘‘centrally condensed’’ polytrope: a polytropic sphere with a point mass in its center. This is a less accurate approximation than it is for a red giant, since deuterium shell burning in a protostar only expands the envelope by a factor of slightly more than 2, as opposed to more than an order of magnitude for a red giant. However, we can regard the pure polytropic model of a star before shell burning and the centrally condensed polytropic model for a star during shell burning as limiting cases.

Centrally condensed $n = 3/2$ polytropes obey a mass-radius relation (Paczyński & Sienkiewicz 1972)

$$R = KE^{2/3} M^{-1/3}, \quad (5)$$

where K is a constant that depends on the specific entropy in the convective envelope and E is a dimensionless number that depends only on ξ , the ratio of the core mass to the total mass. Since the star behaves adiabatically as mass is removed, K remains constant. If the mass of the radiative core is also unchanged, a

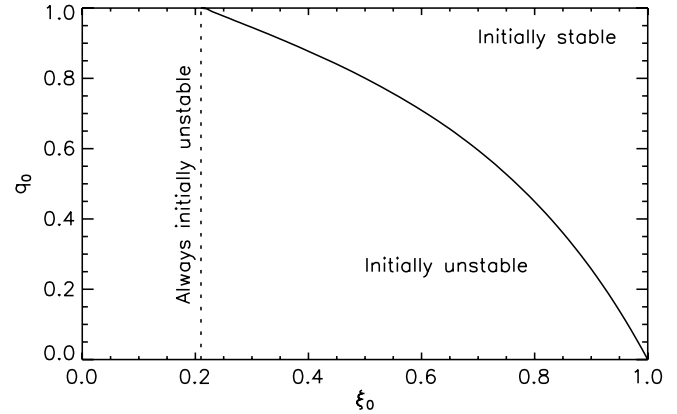


FIG. 3.—Minimum initial mass ratio q_0 required to make mass transfer stable for a given initial core mass fraction ξ_0 . The dotted line at $\xi_0 = 0.22$ indicates the minimum ξ_0 below which mass transfer is always unstable, regardless of the value of q_0 .

reasonable approximation when transfer begins, then the radius of the star varies as

$$\frac{\dot{R}_{*1}}{R_{*1}} = -\frac{\dot{M}_1}{3M_1} \left\{ 1 + 2 \left[\frac{\xi_0}{E(\xi_0)} \right] \frac{dE}{d\xi} \Big|_{\xi=\xi_0} \right\}, \quad (6)$$

where ξ_0 is the core mass ratio at the start of mass transfer. The star expands for $\xi_0 < 0.22$ and shrinks for $\xi_0 > 0.22$.

Since $R_{r1} = R_{*1}$ at the start of mass loss, mass transfer is unstable unless $\dot{R}_{*1} < \dot{R}_{r1}$. This condition is met only if

$$\frac{1}{3} \left\{ 1 + 2 \left[\frac{\xi_0}{E(\xi_0)} \right] \frac{dE}{d\xi} \Big|_{\xi=\xi_0} \right\} < (1 - q_0) \left[\frac{2}{q_0} + \frac{2 \log(1 + q_0^{-1/3}) - (1 + q_0^{1/3})^{-1}}{1.8q_0^{1/3} + 3q_0 \log(1 + q_0^{-1/3})} \right]. \quad (7)$$

By evaluating E and $dE/d\xi$ numerically (e.g., Table 1 of Paczyński & Sienkiewicz 1972), this condition lets us identify for each ξ_0 what values of the initial mass ratio q_0 produce stability. Figure 3 shows that for $\xi_0 < 0.22$, no stability is possible because the star expands rather than contracts in response to mass loss.

Stars without radiative cores have $\xi = 0$, so if RLOF occurs before the onset of shell burning, then $\xi_0 = 0$ and the transfer is unstable. Shell burning stars will have $\xi_0 > 0$, and they may be stable if ξ_0 and q_0 are large enough. The value of ξ_0 is determined by the size of the radiative core when it first appears, which is in turn set by the radius of the shell where the maximum luminosity that can be transported by radiation, $L_{\text{rad}}(m)$, first rises to the point where it is equal to the luminosity passing through that shell, $L(m)$. Here, m is the mass enclosed within a given shell and varies from $m = 0$ at the center of the star to $m = M_1$ at its surface.

From their numerical models, Palla & Stahler (1992) find that $L_{\text{rad}}(m) = L(m)$ is first satisfied at $m/M_1 = \xi_0 = 0.20, 0.21,$ and 0.41 for accretion rates of $10^{-5}, 3 \times 10^{-5},$ and $10^{-4} M_\odot \text{ yr}^{-1}$. We would like to extrapolate to higher accretion rates, but that is quite difficult because ξ_0 varies so nonlinearly with $M_{1,\text{acc}}$. Instead, we make some general observations to help understand the likely value of ξ_0 . The nonlinearity in the variation of ξ_0 with $M_{1,\text{acc}}$ results from the complicated shape of $L_{\text{rad}}(m)$ (see Fig. 5 of Palla & Stahler 1991). This shape admits two possible solutions

to $L_{\text{rad}}(m) = L(m)$, i.e., two mass shells where a convectively stable zone could appear, one at smaller m and one at larger m . The reason ξ_0 is nearly unchanged between $\dot{M}_{1,\text{acc}} = 10^{-5}$ and $3 \times 10^{-5} M_{\odot} \text{ yr}^{-1}$ is that $L_{\text{rad}}(m) = L(m)$ is first satisfied at the same solution point in the two models; ξ_0 jumps between $\dot{M}_{1,\text{acc}} = 3 \times 10^{-5}$ and $10^{-4} M_{\odot} \text{ yr}^{-1}$ because the point where $L_{\text{rad}}(m)$ and $L(m)$ first become equal moves from the inner to the outer possible solution. Since the shape of the $L_{\text{rad}}(m)$ curve does not suggest that there are other, larger mass solutions where $L_{\text{rad}}(m) = L(m)$ might first occur, it seems unlikely that ξ_0 will be much larger than 0.41. However, we caution that this is a tentative conclusion, and that one cannot confidently estimate ξ_0 without detailed numerical modeling. In particular, the value of ξ_0 in the models of Palla & Stahler (1991, 1992) appears to be sensitive to their choice of boundary condition.

If our tentative conclusion holds and $\xi_0 \lesssim 0.5$ regardless of the accretion rate, then transfer will be unstable unless $q_0 \gtrsim 0.8$.

3.3. The Fate of Stable Mass Transfer Binaries

Massive binary systems that initiate stable mass transfer lie in the region of parameter space above the line in Figure 3. Stable transfer is possible only if it starts because the more massive star has initiated shell burning and possesses a radiative core. While transfer reduces the temperature in the envelope via adiabatic expansion and thus halts shell burning immediately, this seems likely to produce only a temporary reprieve. As the primary continues to contract toward the main sequence on a Kelvin-Helmholtz timescale, it cannot avoid reheating and again igniting deuterium in its envelope, producing further expansion. Thus, there may be multiple episodes of shell burning, expansion, and stable mass transfer separated by time intervals of order τ_{KH} , each leading to the transfer of a relatively small amount of mass, but accumulating over time to push the system considerably toward $q = 1$. Determining the detailed evolution of a system undergoing this process requires the ability to follow the internal structure of the donor star as it repeatedly loses small amounts of gas from its envelope, cools adiabatically, and then heats up again. This is beyond the capabilities of our simple protostellar evolution model, and since our best estimate for ξ_0 indicates that the unstable mass transfer is likely to be a more common occurrence than stable transfer, we do not pursue the problem further in this paper.

3.4. Termination of Unstable Mass Transfer

We have found that unless the mass ratio is already near unity and the donor star is shell burning, mass transfer is unstable and proceeds on a dynamical timescale. This makes it difficult to determine the precise outcome without a protostellar model that, unlike ours, is capable of following the accretion of very high entropy gas on this timescale. Numerical simulations of the transfer itself would also be helpful, since in the case of runaway transfer it is possible that mass lost from the primary may go into a circumbinary disk or a wind, rather than accreting onto the secondary. Nonetheless, we can make some simple calculations to estimate how and whether mass transfer will cease.

Mass transfer will continue until either the primary shrinks within its Roche lobe or the secondary overflows its Roche lobe too. We discuss the latter outcome in § 3.5. We can check whether the former is a possibility by asking whether there exists a new mass ratio q , larger than the original mass ratio q_0 , such that the primary and secondary are both within their Roche lobes. Since such an equilibrium must be established on the dynamical timescale, the donor star must be able to reach it adiabatically. To

determine whether such an equilibrium exists, we first examine how the Roche radius and stellar radius for each star change with q in § 3.4.1, and then we search for equilibria in § 3.4.2.

3.4.1. Roche Radius and Stellar Radius

If the mass transfer conserves both total system mass and angular momentum, then the ratio of the semimajor axis a to its value a_0 before transfer starts is

$$\frac{a}{a_0} = \left(\frac{q_0}{q}\right)^2 \left(\frac{1+q}{1+q_0}\right)^4 \quad (8)$$

when the mass ratio reaches q . From equation (1), the new Roche radius of the primary is related to the original one, $R_{r1,0}$, by

$$\frac{R_{r1}}{R_{r1,0}} = \left(\frac{q_0}{q}\right)^2 \left(\frac{1+q}{1+q_0}\right)^4 \left[\frac{0.6 + q_0^{2/3} \log(1 + q_0^{-1/3})}{0.6 + q^{2/3} \log(1 + q^{-1/3})} \right]. \quad (9)$$

The ratio of current to initial Roche radius for the second star, $R_{r2}/R_{r2,0}$, is given by an equivalent expression with q and q_0 replaced with q^{-1} and q_0^{-1} , respectively. Note that once mass transfer on a dynamical timescale begins, the two stars cannot remain exactly synchronous, nor can they be treated as point masses, and thus equations (8) and (9) are approximate (J. Goodman 2007, private communication).

Similarly, from the mass-radius relation (eq. [5]), the initial radius of star 1 and its radius once the mass ratio reaches q are related by

$$\frac{R_{*1}}{R_{*1,0}} \approx \left(\frac{1+q}{1+q_0}\right)^{1/3} \left(\frac{E\{[(1+q)/(1+q_0)]\xi_0\}}{E(\xi_0)}\right)^{2/3}. \quad (10)$$

This relation will break down if $\xi = \xi_0(1+q)/(1+q_0)$ becomes too large, because formally a centrally condensed polytrope goes to zero radius as $\xi \rightarrow 1$. In reality, the radiative core has a finite radius, which the simulations of Palla & Stahler (1991, 1992) show is $\sim 1/2$ of a dex smaller than the total stellar radius at the onset of shell burning. However, we find below that the radius of the primary star can never become this small before the secondary overflows its Roche lobe, so equation (10) is an adequate approximation for our purposes.

Now consider the secondary star. Mass transferred from the primary to the secondary will not have time to cool and will therefore retain its specific entropy; it may even gain entropy due to an accretion shock as it falls onto the secondary. Since this high-entropy material is being transferred to the smaller potential well of the second star, it will rapidly expand the secondary's radius and eventually cause it to overflow its Roche lobe as well.

We can obtain a rough lower bound on the secondary's radius by treating it as a centrally condensed polytrope as well. In this approximation, we take the secondary's radius at the onset of transfer to be negligible in comparison to its radius after mass transfer starts, and thus treat the secondary at the start of transfer as a point mass. After an amount of mass ΔM has been transferred, the secondary has mass $M_2 = M_{2,0} + \Delta M$ and envelope-to-core mass ratio $\xi_2 = \Delta M/M_{2,0}$. Since the specific entropy of the gas that is transferred is the same as or larger than it was before the transfer, the constant K for the secondary is at a minimum the same as for the primary at the onset of transfer,

$$K = R_{*1,0} M_{1,0}^{1/3} E(\xi_0)^{-2/3} = R_{r1,0} M_{1,0}^{1/3} E(\xi_0)^{-2/3}. \quad (11)$$

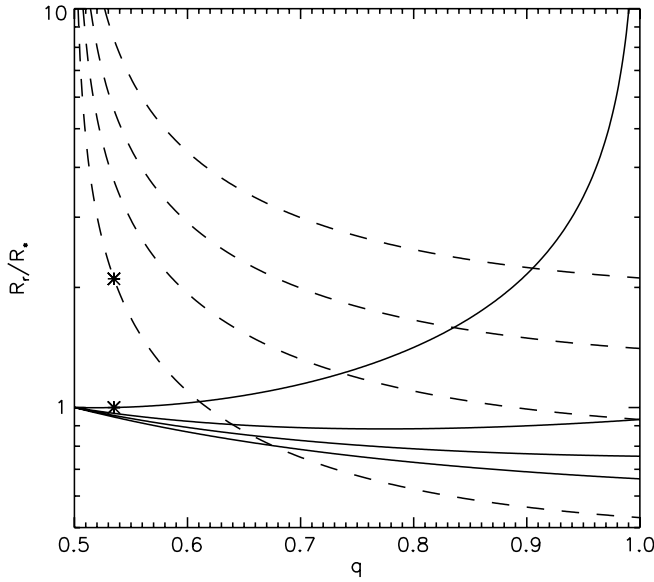


FIG. 4.—Ratio of Roche radius R_r to stellar radius R_* for the primary star (solid lines) and the secondary star (dashed lines) for a system with $q_0 = 0.5$ initially. We show curves for $\xi_0 = 0, 0.25, 0.5,$ and 0.75 , from lowest to highest. A system stabilizes if there is a value of q for which $R_r/R_* > 1$ for both stars. The asterisks mark an example of such a stable point: a system with $q_0 = 0.5$ and $\xi_0 = 0.75$ stabilizes at $q = 0.54$.

The radius of the secondary is therefore bounded below by

$$R_{*2} > R_{*1,0} \left[\frac{1+q}{(1+q_0)q} \right]^{1/3} \left(\frac{E\{[q_0/q][(1+q)/(1+q_0)]\}}{E(\xi_0)} \right) \quad (12)$$

at the point when the mass ratio is q .

3.4.2. Existence of Mechanical Equilibria

Having determined how the Roche radius and stellar radius for each star vary as the stars exchange mass and q changes, we are now in a position to determine whether there is a state that the system can reach adiabatically in which neither star is overflowing its Roche lobe. Such an equilibrium exists if and only if there is a value $q > q_0$ such that $R_{*1} \leq R_{r1}$ and $R_{*2} \leq R_{r2}$. We also require $q \leq 1$. Since the envelope of the primary has higher entropy than that of the secondary, the secondary will certainly overflow its Roche lobe by the time $q = 1$ is reached, even though our lower limit in equation (12) does not reflect this. We illustrate an example of the problem graphically in Figure 4, which shows the ratio of Roche radius to stellar radius for both stars as a function of q for $q_0 = 0.5$ and various values of ξ_0 .

As the figure shows, for a given value of q_0 and ξ_0 , there may or may not be a value of q satisfying the condition that both stars are within their Roche radii. If there is such a q , then mass transfer will halt once the system reaches that value. We summarize these results in Figure 5, which shows the value of q for which a system stabilizes as a function of q_0 and ξ_0 . In the upper right white region of the plot, systems are initially stable and mass transfer does not occur on a dynamical timescale (see § 3.3). In the lower left region, systems are always unstable and there is no value of q for which the donor star can shrink within its Roche lobe. Systems whose parameters fall within the shaded region in between are initially unstable, but can stabilize and stop transferring mass for some value of q . Generically, we find that systems are unable to reach equilibrium unless they fall within a

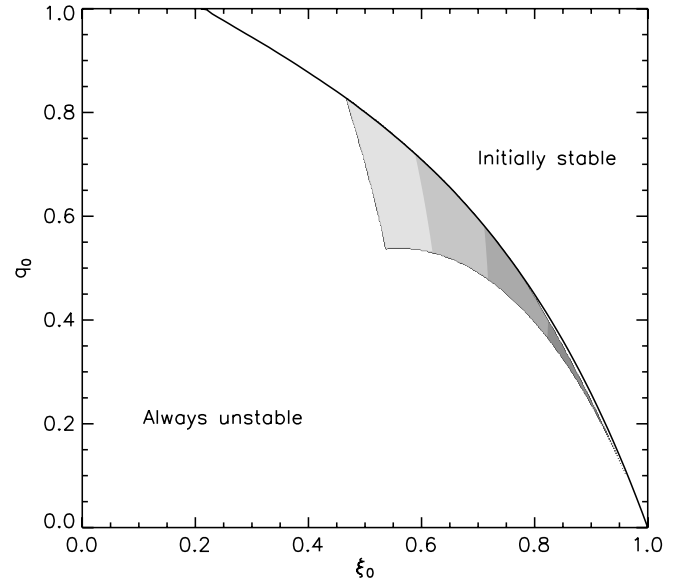


FIG. 5.—Value of q for which mass transfer terminates, as a function of ξ_0 and q_0 . Outside the shaded region, either mass transfer is always stable (top right region) or there is no value of q for which it will terminate (bottom left region). Inside the shaded region, the gray-scale shows the value of q for which mass transfer terminates. The lightest region corresponds to $q > 0.8$, the next darkest region to $0.6 < q \leq 0.8$, the next to $0.4 < q \leq 0.6$, and so forth. Although ξ_0 is uncertain, in § 3.2 we argue on the basis of the models of Palla & Stahler (1991, 1992) that it is likely to be ≤ 0.5 .

relatively small region of parameter space. Note that even this certainly overestimates the size of the stable region, since our estimate for R_{*2} is only a lower limit. Thus, once transfer starts, it generally continues until both stars overflow their Roche lobes.

3.5. The Fate of Unstable Mass Transfer Binaries

What is the fate of a mass transfer binary in which the primary cannot shrink inside its Roche lobe before the secondary also overflows its Roche lobe? Such a system will become a contact binary, or possibly even a common envelope system if the semimajor axis decreases enough. Equation (8) implies that in a binary that transfers enough mass to reach $q = 1$, the semimajor axis shrinks by a factor of $2^4 q_0^2 / (1+q_0)^4$. For $q_0 = 0.1$, this is a factor of 10, and almost certainly produces common envelope evolution, or possibly even a merger. However, for $q_0 = 0.5$, the change in separation is only 20%, so a contact binary seems the more likely outcome.

Once a contact binary or common envelope forms, over a thermal time the envelopes of stars will equilibrate to the same specific entropy. If the primary has a radiative core it will not equilibrate, but the radiative core may well disappear temporarily, because as it expands and cools adiabatically, its opacity will increase, and it may transition back to convective instability. If this happens, it will reach the same specific entropy as the two envelopes. The result will be an entirely isentropic contact binary. Since the two stars are isentropic, gas will be equally strongly bound to each of the two potential wells, and the system will approach equal masses. As the stars radiate, they will continue contracting, their envelopes will shrink, and eventually contact will cease before the stars reach the ZAMS. The result will be a main-sequence detached binary with a mass ratio close to unity.

Note that this behavior is different from that commonly observed in main-sequence or post-main-sequence contact binaries, which do not approach equal masses. In those systems, the two stars are chemically different (e.g., one may have consumed all

of its hydrogen), or one or both may contain degenerate cores that will not reach the same specific entropy as the envelopes. It is these differences that produce unequal masses.

After contact ceases and the stars contract to the ZAMS, the orbit will circularize and the binary will become synchronous. The characteristic timescale for the former has been estimated by Goodman & Dickson (1998; their eq. [15]). Taking representative parameters, the circularization timescale for an equal-mass binary with separation $a \sim 0.1$ AU and constituent masses of $10 M_{\odot}$ and radii $R \sim 0.02$ AU is $t_{\text{circ}} \sim 10^2 \text{ yr } (R/0.02 \text{ AU})^{3/2} [(a/R)/5]^{21/2}$. The very strong dependence on the ratio a/R makes this estimate quite uncertain: a factor of 2 change in a/R increases t_{circ} by a factor of 10^3 . Importantly, however, the timescale is shorter than or comparable to the characteristic thermal time. The synchronization timescale (t_{syn}) can be estimated from the work of Goldreich & Nicholson (1989). Using the same parameters as for the estimation of t_{circ} , we find a synchronization timescale of $t_{\text{syn}} \sim t_{\text{circ}}$, again with a similar and very strong dependence on the magnitude of a/R . Although uncertain, these estimates indicate that close massive binaries should be synchronous and on circular orbits relatively early in their main-sequence lifetimes.

4. DISCUSSION

A primary result of this work is that there is a critical a below which RLOF occurs (eq. [2]; Fig. 2). Thus, for massive binaries that form at a separation of a few tenths of an AU, RLOF and mass transfer occur before either star reaches the ZAMS. For a relatively wide range of parameter space, mass transfer is unstable, and we argue that the binary mass ratio will be driven toward equality on a dynamical timescale. For high system accretion rates, the ratio of the radiative core mass to the envelope mass of the primary protostar (ξ_0) can be ~ 0.5 , and in some cases the system can stabilize for some values of $q < 1$. Somewhat unequal mass binaries are the result when the stars reach the ZAMS (Fig. 5).

4.1. “Twin” Binaries

A particularly curious feature of the massive binary population is the high proportion of systems with mass ratios very close to unity. The mass ratio of WR 20a is $q = 0.99 \pm 0.05$ (Bonanos et al. 2004; Rauw et al. 2005), and that of D33 J013346.2+304439.9 is $q = 0.90 \pm 0.15$ (Bonanos et al. 2006). Thirteen of the 21 detached binaries in the Hilditch et al. (2005) sample have $q > 0.85$, and five have best-fit values of q consistent with $q = 1.0$ (Pinsonneault & Stanek 2006). Due to its small size, the statistical significance of this sample is unclear (Lucy 2006), but a priori it seems quite unusual that almost 25% of the eclipsing binaries in the SMC with orbital periods shorter than 5 days should have mass ratios consistent with 1.0. Nor does it seem likely a priori that the most massive binary known should have a mass ratio within 5% of unity.

Accretion from a circumbinary disk, as in the model of Bate (2000), provides a way of producing an anticorrelation between semimajor axis and binary mass ratio, such as is observed even for low-mass stars (Tokovinin 2000). However, to produce mass ratios near unity, this mechanism requires that binary protostars initially form with very small masses and then accrete many times their original mass from a circumbinary disk. While such low mass seeds may form in the cold, lower density cores from which low-mass stars form, both analytic work (Krumholz 2006) and simulations (Krumholz et al. 2007) suggest that radiation feedback largely prevents the formation of small “seed” stars in massive protostellar cores. In the simulations of Krumholz et al. (2007), secondaries may form by fragmentation out of a mas-

sive unstable disk (with subsequent migration) or via capture of a fragment formed elsewhere in the core, but in either case the primary at the time of binary formation is at least a few M_{\odot} in mass, and the secondary is at least a few tenths of M_{\odot} . Such a system likely could not reach a mass ratio of unity via the Bate mechanism. However, as we have shown here, mass transfer between massive accreting protostars provides a natural, and for close binaries inevitable, mechanism for attaining mass ratios near unity. That said, the circumbinary accretion mechanism of Bate probably operates in tandem with mass transfer—particularly at lower masses—bringing binaries closer together and pushing mass ratios to larger values before mass transfer occurs and produces a q of nearly 1.0 for tight binaries.

4.2. Observational Predictions

These calculations lead to definite predictions about the properties of massive binaries, which will be directly testable against future samples of binary systems larger than those available today. Since there is both a critical mass and a critical semimajor axis required for RLOF to occur, we predict that true twins, systems with mass ratios $q > 0.95$, should be significantly more common among stars with masses $\gtrsim 5\text{--}10 M_{\odot}$ and semimajor axes $\lesssim 0.25$ AU than among a binary population with either lower mass or larger separation. These twins should be in nearly zero eccentricity orbits, since mass transfer and evolution into a contact binary will circularize orbits rapidly.

Furthermore, systems with small values of q_0 that begin mass transfer will experience large reductions in the system semimajor axis. For example, a system with $q_0 = 0.1$ will reduce its separation by a factor of 10, likely producing a merger. This may lead to a deficit of low-mass companions to massive stars at separations significantly smaller than a tenth of an AU. Unfortunately, predictions regarding close binaries with small q are very hard to test observationally because such systems are difficult to detect.

Massive stars should generally have larger mass ratios in clusters with high surface density, since these likely formed from higher pressure gas and thus produced larger accretion rates onto the stars within them (McKee & Tan 2003). However, this effect is likely to be rather weak, since the critical semimajor axis only varies with the quarter power of accretion rate, and very high accretion rates make it easier for stars to remain of unequal mass after the onset of transfer because they decrease the fraction of the star’s mass that goes into the extended envelope. As a result, there may be fewer true twins in very high surface density systems, even if there are more massive stars with mass ratios $\gtrsim 0.5$. In any event, due to weak dependence on the accretion rate, we consider this possibility less promising than searching for correlations of twin fraction with mass and semimajor axis.

4.3. Primordial Stars

One final note is that although we have not discussed primordial stars, the mechanism we have discussed may well operate in them too. The critical ingredients for mass transfer are a phase of deuterium shell burning to produce large radii and a close companion onto which to transfer mass. The binary properties of primordial stars are completely unknown, so we cannot comment on whether the second condition is likely to be met. However, a phase of deuterium shell burning does seem likely. Primordial stars probably form at high accretion rates (Tan & McKee 2004), giving them large radii (Stahler et al. 1986). In present-day stars, a radiative barrier forms because opacity in a stellar interior decreases with temperature. The opacity source is primarily free-free transitions of electrons, and the availability of electrons for this process does not depend strongly on metallicity in an ionized

stellar interior. Thus, primordial stars likely form radiative barriers much like present-day ones, and undergo deuterium shell burning.

5. SUMMARY

Massive, rapidly accreting protostars can reach radii of tenths of an AU during their pre-main-sequence evolution, largely because they undergo a phase of deuterium shell burning that swells their radii. During this evolutionary phase, massive protostars with close companions will overflow their Roche lobes and transfer mass. Such transfer is always from the more massive, rapidly accreting star to the smaller one, since radius increases with both mass and accretion rate. Using simple protostellar structure and evolution models, we evaluate the range of separations and mass ratios for which mass transfer is expected to occur and compute the likely outcome of the transfer.

We find that for the expected accretion rates in massive star-forming regions, binaries at separations of several tenths of an AU or closer will undergo mass transfer, with some dependence on the exact accretion rate and the initial mass ratio. This process always pushes binaries toward mass ratios of unity. For some accretion rates and initial mass ratios, mass transfer either will be stable initially or will terminate on its own before reaching $q = 1$. For many systems, however, it will only halt when the two stars form a contact binary. The stellar envelopes in such systems will rapidly reach almost equal masses and specific entropies, and the stars will then contract onto the main sequence, forming a ZAMS binary with a mass ratio very close to unity.

Pre-main-sequence mass transfer represents a heretofore unknown phase of binary star formation and evolution, one that has likely affected a significant fraction of massive spectroscopic binaries. It provides a natural explanation for the puzzling phenomenon of massive twins, high-mass binaries with mass ratios that are consistent with $q = 1.0$. We predict based on this finding that twins should be significantly more common among stars $\geq 5-10 M_{\odot}$ in mass at separations ≤ 0.25 AU than among either less massive or more distant stars, and that mass ratios should generally increase with binary mass and decrease with separation. The weak dependence of a_{crit} in equation (2) on the system mass accretion rate and the initial mass ratio suggests that this result should not depend significantly on formation environment. Surveys, such as OGLE, that detect statistically large samples of massive binaries are rapidly making these predictions testable.

We thank J. Goodman, S. W. Stahler, and J. M. Stone for discussions and helpful comments on the manuscript, and B. Paczyński for prompting us to think about this problem. M. R. K. acknowledges support from NASA through Hubble Fellowship grant HSF-HF-01186 awarded by the Space Telescope Science Institute, which is operated by the Association of Universities for Research in Astronomy, Inc., for NASA, under contract NAS 5-26555. T. A. T. acknowledges support from a Lyman Spitzer Jr. Fellowship.

REFERENCES

- Apai, D., Bik, A., Kaper, L., Henning, T., & Zinnecker, H. 2007, *ApJ*, 655, 484
 Banerjee, R., & Pudritz, R. E. 2007, *ApJ*, 660, 479
 Bate, M. R. 2000, *MNRAS*, 314, 33
 Bonanos, A. Z., et al. 2004, *ApJ*, 611, L33
 ———. 2006, *ApJ*, 652, 313
 Bonnell, I. A., & Bate, M. R. 2005, *MNRAS*, 362, 915
 Bonnell, I. A., Bate, M. R., & Zinnecker, H. 1998, *MNRAS*, 298, 93
 Eggleton, P. P. 1983, *ApJ*, 268, 368
 Goldreich, P., & Nicholson, P. D. 1989, *ApJ*, 342, 1079
 Goodman, J., & Dickson, E. S. 1998, *ApJ*, 507, 938
 Harries, T. J., Hilditch, R. W., & Howarth, I. D. 2003, *MNRAS*, 339, 157
 Henning, T., Schreyer, K., Launhardt, R., & Burkert, A. 2000, *A&A*, 353, 211
 Hilditch, R. W., Howarth, I. D., & Harries, T. J. 2005, *MNRAS*, 357, 304
 Keto, E., & Wood, K. 2006, *ApJ*, 637, 850
 Kratter, K. M., & Matzner, C. D. 2006, *MNRAS*, 373, 1563
 Krumholz, M. R. 2006, *ApJ*, 641, L45
 Krumholz, M. R., Klein, R. I., & McKee, C. F. 2007, *ApJ*, 656, 959
 Lada, C. J. 2006, *ApJ*, 640, L63
 Lucy, L. B. 2006, *A&A*, 457, 629
 McKee, C. F., & Tan, J. C. 2003, *ApJ*, 585, 850
 Paczyński, B., & Sienkiewicz, R. 1972, *Acta Astron.*, 22, 73
 Palla, F., & Stahler, S. W. 1991, *ApJ*, 375, 288
 ———. 1992, *ApJ*, 392, 667
 Pinsonneault, M. H., & Stanek, K. Z. 2006, *ApJ*, 639, L67
 Preibisch, T., Weigelt, G., & Zinnecker, H. 2001, in *IAU Symp. 200, The Formation of Binary Stars*, ed. H. Zinnecker & R. Mathieu (Cambridge: Cambridge Univ. Press), 69
 Rauw, G., et al. 2005, *A&A*, 432, 985
 Shatsky, N., & Tokovinin, A. 2002, *A&A*, 382, 92
 Stahler, S. W. 1988, *ApJ*, 332, 804
 Stahler, S. W., Palla, F., & Salpeter, E. E. 1986, *ApJ*, 302, 590
 Tan, J. C., & McKee, C. F. 2004, *ApJ*, 603, 383
 Tokovinin, A. A. 2000, *A&A*, 360, 997
 Udalski, A., Soszynski, I., Szymanski, M., Kubiak, M., Pietrzynski, G., Wozniak, P., & Zebrun, K. 1998, *Acta Astron.*, 48, 563